



Supplement of

Radical chemistry in the Pearl River Delta: observations and modeling of OH and HO₂ radicals in Shenzhen in 2018

Xinping Yang et al.

Correspondence to: Keding Lu (k.lu@pku.edu.cn) and Yuanhang Zhang (yhzhang@pku.edu.cn)

The copyright of individual parts of the supplement might differ from the article licence.

17 **Table S1: Information on the instruments at Shenzhen in the autumn of 2018.**

Parameters	Measurement technique	Time resolution	Detection limit ^a	Accuracy
OH	LIF ^b	30 s	$5.0 \times 10^5 \text{ cm}^{-3}$	$\pm 11\%$
HO ₂	LIF ^{b,c}	30 s	$1.0 \times 10^7 \text{ cm}^{-3}$	$\pm 15\%$
<i>k</i> _{OH}	LP-LIF ^d	5 min	(1.5-2.0) s ⁻¹	$\pm 10\%$
Photolysis frequencies	Spectroradiometer	10 s	^e	$\pm 5\%$
O ₃	UV photometry	60 s	500 ppt	$\pm 5\%$
NO	Chemiluminescence	60 s	50 ppt	$\pm 10\%$
NO ₂	Chemiluminescence ^f	60 s	50 ppt	$\pm 10\%$
HONO	LOPAP ^g	60 s	12 ppt	$\pm 20\%$
CO	IR absorption	60 s	50 ppt	$\pm 5\%$
SO ₂	Pulsed UV fluorescence	60 s	100 ppt	$\pm 10\%$
HCHO	Hantzsch fluorimetry	60 s	25 ppt	$\pm 5\%$
VOCs ^h	GC-MS/FID ⁱ	1 h	(20-300) ppt	$\pm 15\%$

18 Note that:

19 ^a Signal-to-noise ratio = 1. ^b Laser-Induced Fluorescence. ^c Chemical conversion via NO reaction before detection. ^d Laser
 20 Photolysis-Laser Induced Fluorescence. ^e Process-specific, 5 orders of magnitude lower than the maximum at noon. ^f
 21 Photolytic conversion to NO before detection, home-built converter. ^g Long-path absorption photometry. ^h C₂-C₁₂ VOCs. ⁱ
 22 Gas Chromatography with Mass Spectrometry / with Flame Ionization Detection.

23

24 **The evaluation of the potential interference in OH measurements**

25 We compared the environmental conditions in Shenzhen and Wangdu sites. The chemical modulation tests, which was
 26 applied to test the potential OH interference, were conducted on 29 June, 30 June, 02 July and 05 July 2014 in Wangdu (Tan
 27 et al., 2017). During the campaign in Wangdu, the daily mean O₃, alkenes (ethene, butadiene and other anthropogenic dienes,
 28 internal alkenes and terminal alkenes) and isoprene concentrations during the daytime on 29 June were 94.1, 3.8, 1.9 ppb,
 29 those on 30 June were 92.2, 2.7, and 1.9 ppb, those on 02 July were 52.9, 1.5, and 0.5 ppb, and those on 05 July were 68.5,
 30 2.4, and 0.9 ppb, respectively. The O₃, alkenes and isoprene concentrations on 29 June were the highest among those on 29
 31 June, 30 June, 02 July and 05 July, and thus the potential interference on 29 June can be considered the highest among the
 32 four days. The chemical modulation results indicated that the potential interference during the daytime in Wangdu was
 33 negligible (Tan et al., 2017).

34 As shown in Table S2, the O₃, alkenes and isoprene concentrations in Shenzhen were within 8.6-91.7 ppb, 1.2-5.4 ppb,
 35 and 0.1-1.0 ppb, respectively. The O₃ concentrations in Shenzhen (8.6-91.7 ppb) were lower than those on 29 June (94.1 ppb)
 36 and 30 June (92.2 ppb) in Wangdu. Similarly, the isoprene concentrations in Shenzhen (0.1-1.0 ppb) were also lower than
 37 those on 29 June (1.9 ppb) and 30 June (1.9 ppb) in Wangdu. In terms of the alkenes, only the concentrations on 10, 16-17
 38 October 2018 (4.7-5.4 ppb) in Shenzhen were higher than that observed on 29 June (3.8 ppb) in Wangdu, but the O₃
 39 concentrations on the three days in Shenzhen were only 21.9, 13.9, and 8.6 ppb, and the isoprene concentrations on the three
 40 days in Shenzhen were only 0.3, 0.2, and 0.1 ppb, respectively.

41 Overall, the environmental condition in Shenzhen was less conducive to generating potential OH interference than that in
 42 Wangdu. Therefore, it is not expected that OH measurement in this campaign was affected by internal interference.

43 **Table S2: The daily mean O₃, alkenes (ethene, butadiene and other anthropogenic dienes, internal alkenes and
 44 terminal alkenes) and isoprene concentrations during the daytime (08:00-17:00) in the STORM campaign in this**

45 **study.**

Date / Species	10-05	10-06	10-07	10-08	10-09	10-10	10-11	10-12	10-13	10-14	10-15	10-16
O ₃ (ppb)	81.4	83.8	91.7	86.7	48.1	21.9	30.2	42.6	46.8	38.7	40.2	13.9
Alkenes (ppb)	1.4	1.8	3.6	2.3	3.2	5.4	2.9	2.4	2.6	1.4	1.6	4.9
Isoprene (ppb)	0.4	0.4	0.4	0.5	0.4	0.3	0.1	0.3	0.4	0.4	0.6	0.2

46

Date / Species	10-17	10-18	10-19	10-20	10-21	10-22	10-23	10-24	10-25	10-26	10-27	10-28
O ₃ (ppb)	8.6	16.2	39.4	45.8	47.2	25.2	40.9	36.5	55.2	56.5	60.9	60.8
Alkenes (ppb)	4.7	3.2	2.1	1.3	1.2	2.5	2.9	2.7	1.2	3.4	1.7	1.7
Isoprene (ppb)	0.1	0.1	0.5	0.3	0.8	0.8	0.4	0.3	0.5	1.0	0.6	0.8

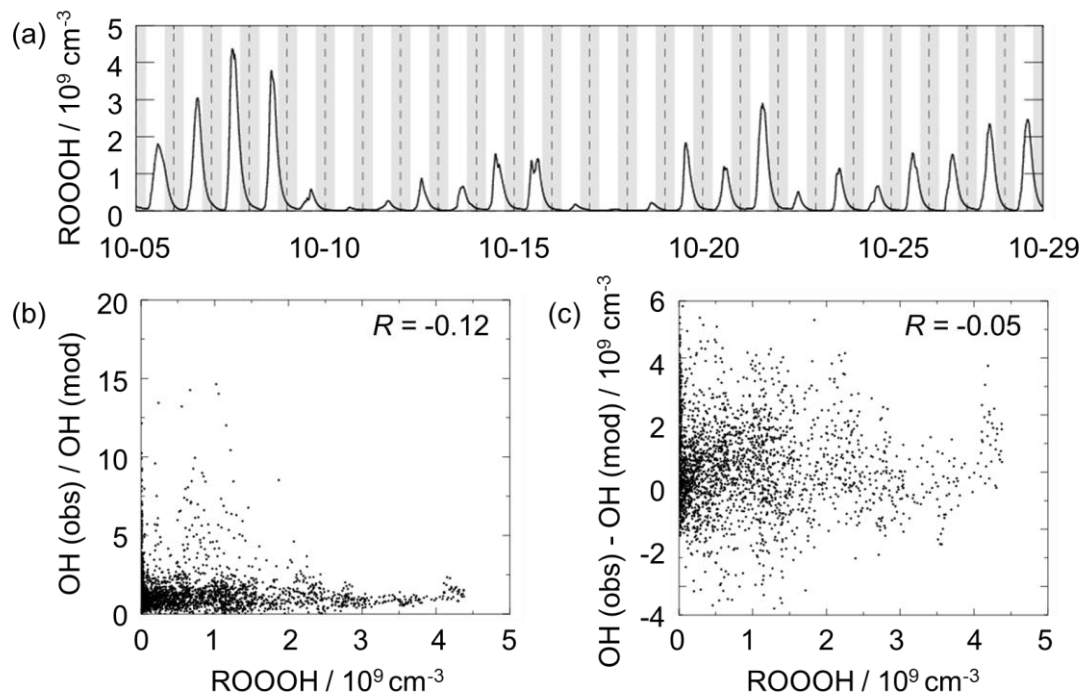
47

48 Additionally, to evaluate the impact of the interference from ROOOH on radical concentrations, we integrated the
 49 reactions of the ROOOH production and destruction into the base model herein, as shown in Eq. (S1-S2).



52 where the RO₂ is across all RO₂ radicals in the model excluding methyl peroxy radicals, for which it has been shown that the
 53 production of a trioxide species is only a minor product channel while the trioxide yield is expected to be close to 1 for larger
 54 peroxy radicals. The rate constant of Eq. (S1) is $1.5 \times 10^{-10} \text{ cm}^3 \text{ s}^{-1}$ (Fittschen et al., 2019). In Eq. (S2), the rate constant is 10^{-4}
 55 s^{-1} , leading to ROOOH lifetimes of around 3 h, of the same order as the lifetime of ROOH species (Fittschen et al., 2019).

56



57

58 **Figure S1: (a) The timeseries of ROOOH concentration from the reactions of RO₂ radicals excluding methyl peroxy**
 59 **radicals with OH radicals. (b) The correlation of the modeled ROOOH concentrations and the ratios of OH**
 60 **observations to OH simulations. (c) The correlation of the modeled ROOOH concentrations and the difference**
 61 **between OH observations and simulations. Only daytime values were chosen in (b-c).**

62

63 **Table S3: The meteorological parameters, photolysis rate constants, and concentrations of trace gases during the**
 64 **campaigns in Backgarden, Heshan, and Shenzhen.**

Parameters	Backgarden (2006, summer)	Heshan (2014, autumn)	Shenzhen (2018, autumn)
Temperature (K)	303.9	295.1	297.5
Pressure (hPa)	1002.9	1010.1	1009.7
Relative humidity (%)	72.3	66	75.4
$j(\text{O}^1\text{D}) / 10^{-5} \text{ s}^{-1}$	3.6	1.3	1.8
$j(\text{NO}_2) / 10^{-3} \text{ s}^{-1}$	7.6	4.1	5.7
CO / ppb	948.6	642.7	386.6
NO / ppb	5.7	3.6	2.6
NO ₂ / ppb	14.3	18.7	14.9
O ₃ / ppb	32.3	26.5	32.2
HONO / ppb	1.0	1.4	0.5
Alkanes / ppb	13.9	16.7	20.2
Alkenes / ppb	2.1	6.0	2.8
Aromatics / ppb	11.2	8.6	8.2
HCHO / ppb	--	5.9	3.3

65

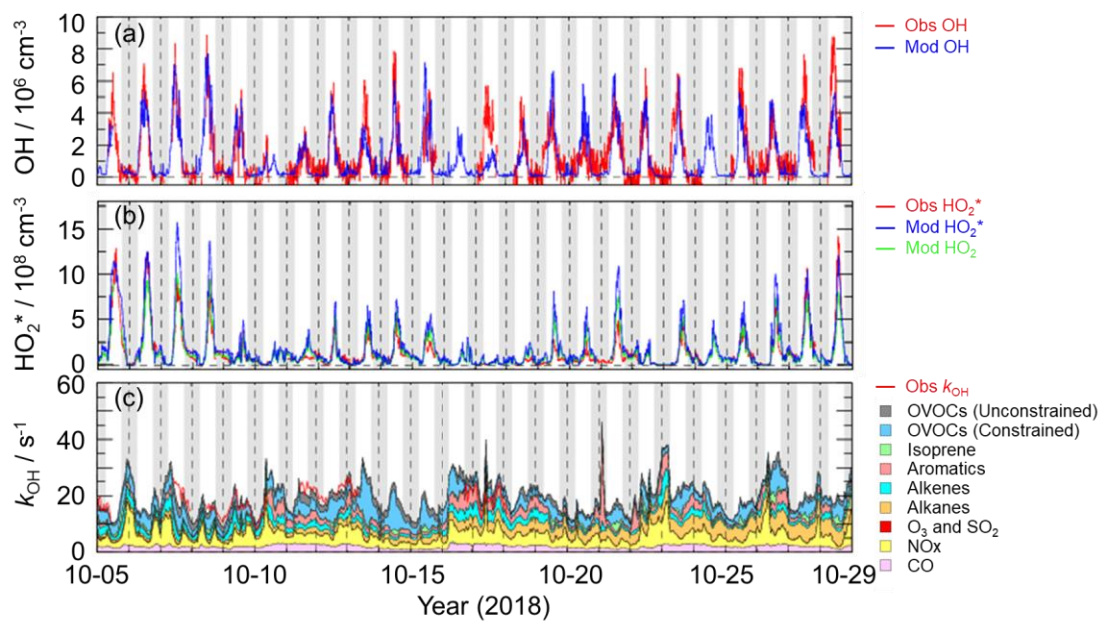
Note that:

66

The $j(\text{O}^1\text{D})$ and $j(\text{NO}_2)$ were the mean values during the noontime, and other parameters were the mean values during the

67

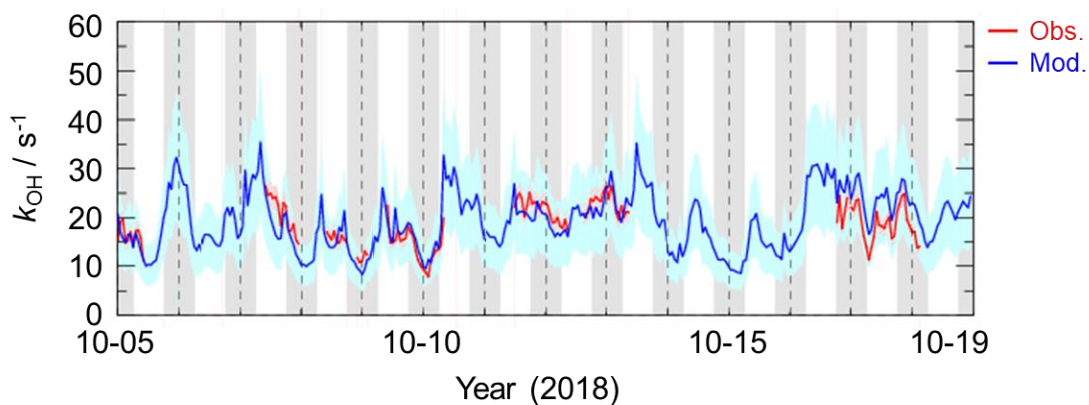
whole day.



69

70 **Figure S2: Timeseries of the OH, HO₂^{*} and HO₂ concentrations, and k_{OH} in this study. The grey areas denote**
 71 **nighttime.**

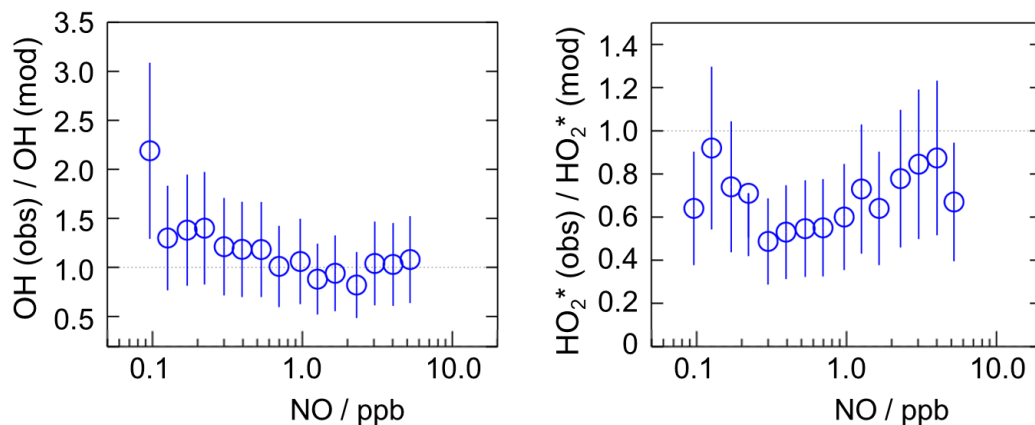
72



73

74 **Figure S3: Timeseries of the observed and modeled k_{OH} during 05-19 October 2018. The red and blue areas denote**
 75 **1- σ uncertainties of the observations and simulations by the model, respectively. The grey areas denote nighttime.**

76



77

78 **Figure S4: NO dependence on the ratios of HOx observations to simulations for daytime conditions. The vertical lines**
 79 **denote the combined uncertainty from radical measurements and model calculations via error propagation.**

80

81 **Table S4: The median values of meteorological and chemical parameters during the daytime at the different NO**
 82 **intervals.**

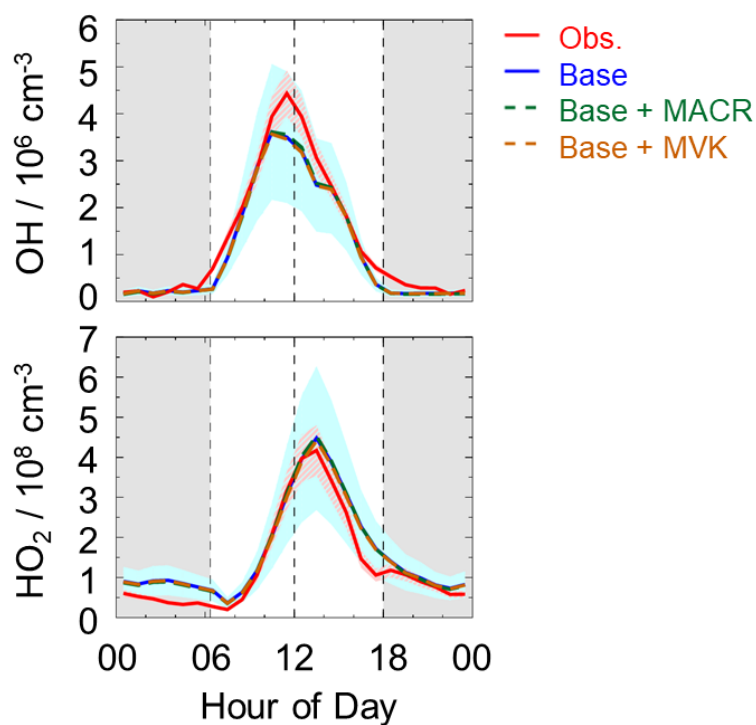
parameters	NO interval	NO interval	NO interval	NO interval
	(< 0.2 ppb)	(0.2-0.6 ppb)	(0.6-2 ppb)	(> 2 ppb)
Temperature / K	301.4	300.8	299.1	297.9
$j(\text{O}^1\text{D}) / 10^{-6} \text{ s}^{-1}$	4.7	8.9	8.2	7.4
O ₃ concentration / ppb	71.7	55.1	39.6	16.9
Alkanes reactivity / s ⁻¹	2.2	3.4	3.3	3.5
Alkenes reactivity / s ⁻¹	1.4	1.0	1.4	2.3
Aromatics reactivity / s ⁻¹	0.9	1.0	1.5	2.4
Isoprene reactivity / s ⁻¹	1.1	1.1	0.8	0.5
HCHO reactivity / s ⁻¹	1.1	0.9	0.8	0.7
ACD reactivity / s ⁻¹	1.1	1.4	1.3	1.2
ACT reactivity / s ⁻¹	0.2	0.2	0.2	0.2
ALD reactivity / s ⁻¹	1.9	1.8	1.6	1.2
KET reactivity / s ⁻¹	0.0	0.0	0.0	0.0
MACR reactivity / s ⁻¹	0.2	0.2	0.1	0.1
MVK reactivity / s ⁻¹	0.3	0.2	0.1	0.1
Modeled OVOCs reactivity / s ⁻¹	2.5	2.2	2.2	2.4
Alkanes concentration / ppb	15.0	16.8	19.0	24.6
Alkenes concentration / ppb	1.6	1.6	2.0	3.4
Aromatics concentration / ppb	3.3	3.3	4.8	7.9

Isoprene concentration / ppb	0.4	0.4	0.3	0.2
HCHO concentration / ppb	5.6	4.3	3.8	3.5
ACD concentration / ppb	3.0	3.7	3.5	3.3
ACT concentration / ppb	3.2	3.7	3.3	2.7
ALD concentration / ppb	3.8	3.6	3.2	2.5
KET concentration / ppb	0.3	0.4	0.4	0.3
MACR concentration / ppb	0.2	0.2	0.1	0.1
MVK concentration / ppb	0.5	0.5	0.3	0.2

83

84

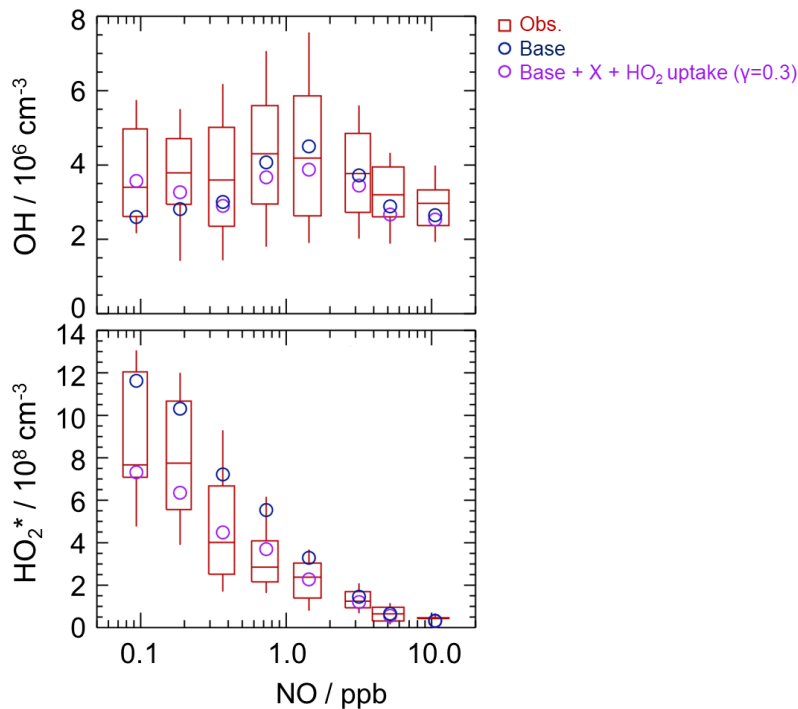
85



86

87 **Figure S5: The diurnal profiles of the observed and modeled radical concentrations. The red lines denote the**
 88 **measured OH and HO₂^{*} concentrations, and the red areas denote 1-σ uncertainties of the measured OH and HO₂^{*}**
 89 **concentrations, respectively. The blue lines denote the modeled OH and HO₂ concentrations by the base model, and**
 90 **the blue areas denote 1-σ uncertainties of the measured OH and HO₂ concentrations, respectively. The green lines**
 91 **denote the OH and HO₂ simulations by the model with the oxidation of MACR, and the dark orange lines denote the**
 92 **OH and HO₂ simulations by the model with the oxidation of MVK. The grey areas denote nighttime.**

93



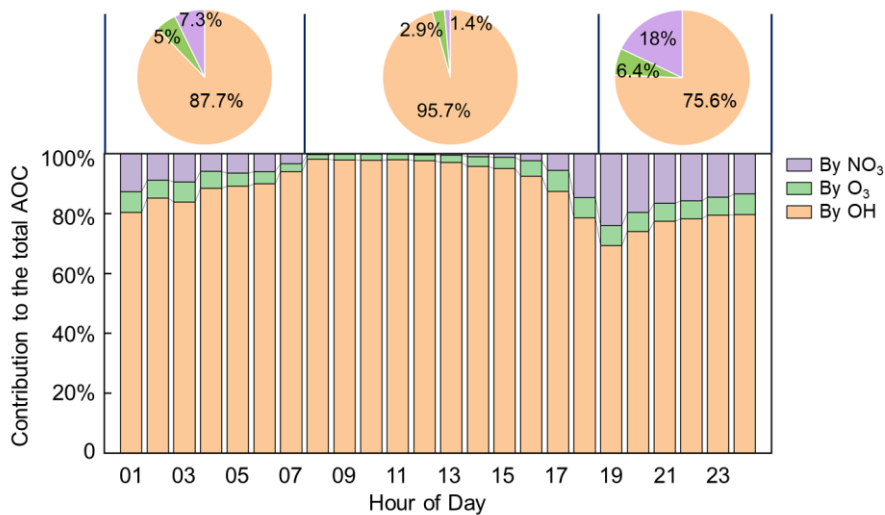
94

95 **Figure S6: NO dependence on OH and HO₂^{*} radicals. The red box-whisker plots give the 10%, 25%, median, 75%,**
 96 **and 90% of the HOx observations. The blue circles show the median values of the HOx simulations by the base model,**
 97 **and the purple circles show the HOx simulations by the model with X mechanism (X = 0.25 ppb NO) and HO₂**
 98 **heterogeneous uptake ($\gamma = 0.3$). Only daytime values and NO concentration above the detection limit of the**
 99 **instrument were chosen.**

100

101

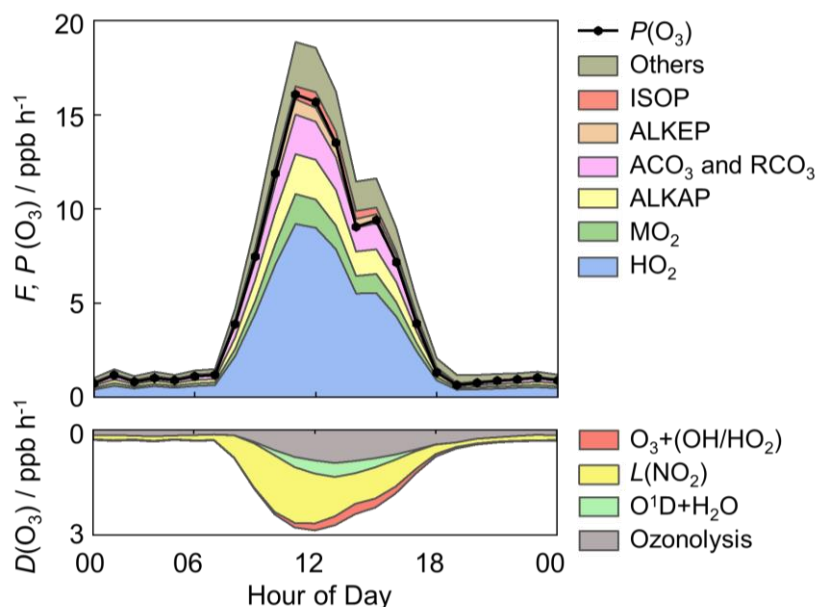
102



103

104 **Figure S7: The Histogram denotes the fractional composition of the total AOC. The left, middle and right pie charts**
 105 **denote the mean contribution of OH, O₃, and NO₃ to the total AOC during the second half of night (00:00-08:00),**
 106 **daytime (08:00-18:00), and the first half of night (18:00-24:00), respectively.**

107



108

109 **Figure S8: The diurnal profiles of $P(O_3)$, $F(O_3)$, and $L(O_3)$ in this campaign. The colored areas denote the speciation**
 110 **of $F(O_3)$ and $L(O_3)$ in the upper panel and lower panel, respectively. The black line denotes the $P(O_3)$, which is the**
 111 **discrepancy between $F(O_3)$ and $L(O_3)$. MO_2 denotes the methyl peroxy radicals. ALKAP, ALKEP and ISOP denote**
 112 **the RO_2 radicals derived from alkanes, alkenes and isoprene, respectively. ACO_3 denotes the acetyl peroxy radicals,**
 113 **and RCO_3 denotes the higher saturated acyl peroxy radicals.**

114

115 **References**

116 Fittschen, C., Al Ajami, M., Batut, S., Ferracci, V., Archer-Nicholls, S., Archibald, A. T., and Schoemaeker, C.: ROOOH: a
 117 missing piece of the puzzle for OH measurements in low-NO environments?, Atmospheric Chemistry and Physics, 19,
 118 349-362, 10.5194/acp-19-349-2019, 2019.

119 Tan, Z., Fuchs, H., Lu, K., Hofzumahaus, A., Bohn, B., Broch, S., Dong, H., Gomm, S., Haeseler, R., He, L., Holland, F., Li,
 120 X., Liu, Y., Lu, S., Rohrer, F., Shao, M., Wang, B., Wang, M., Wu, Y., Zeng, L., Zhang, Y., Wahner, A., and Zhang, Y.:
 121 Radical chemistry at a rural site (Wangdu) in the North China Plain: observation and model calculations of OH, HO2 and
 122 RO_2 radicals, Atmospheric Chemistry and Physics, 17, 663-690, 10.5194/acp-17-663-2017, 2017.

123